

# Ytterbocenes as One- and Two-Electron Reductants in their Reactions with Diazadienes: Yb<sup>III</sup> Mixed-Ligand Bent-Sandwich Complexes Containing a Dianion of Diazabutadiene

Alexander A. Trifonov,<sup>[a]</sup> Ivan A. Borovkov,<sup>[a]</sup> Elena A. Fedorova,<sup>[a]</sup> Georgii K. Fukin,<sup>[a]</sup> Joulia Larionova,<sup>[b]</sup> Nikolai O. Druzhkov,<sup>[a]</sup> and Vladimir K. Cherkasov<sup>[a]</sup>

**Abstract:** Ytterbocene [Yb(C<sub>5</sub>MeH<sub>4</sub>)<sub>2</sub>(thf)<sub>2</sub>] reacts with diazabutadiene 2,6-*i*Pr<sub>2</sub>C<sub>6</sub>H<sub>3</sub>-N=CH-CH=N-C<sub>6</sub>H<sub>3</sub>*i*Pr<sub>2</sub>-2,6 (DAD) as a one-electron reductant to afford a bis(cyclopentadienyl) Yb<sup>III</sup> derivative containing a DAD radical anion [Yb(C<sub>5</sub>MeH<sub>4</sub>)<sub>2</sub>(dad<sup>-</sup>)]. However, ytterbocenes [YbCp\*<sub>2</sub>(thf)<sub>2</sub>] (Cp\* = C<sub>5</sub>Me<sub>5</sub>, C<sub>5</sub>Me<sub>4</sub>H) coordinated by sterically demanding cyclopentadienyl li-

gands act as two-electron reductants in their reactions with DAD. These reactions occur by abstraction of one Cp\* ring and result in the formation of novel Yb<sup>III</sup> mixed-ligand bent-sandwich

complexes, [YbCp\*(dad)(thf)], in which the dianion of DAD has an uncommon terminal η<sup>4</sup>-coordination to the ytterbium atom. The variable-temperature magnetic measurements of complex [Yb(C<sub>5</sub>Me<sub>5</sub>)(dad)(thf)] suggest the existence of redox tautomerism for this compound.

**Keywords:** diazadienes • lanthanides • N ligands • sandwich complexes • ytterbium

## Introduction

Owing to the diversity of their coordination and redox properties, diazabutadiene ligands can provide a promising coordination environment for f transition metals, which can produce unusual structures and contain unique reactivity. Diazabutadienes possess noticeable electron-accepting properties<sup>[1]</sup> and tend to oxidize electropositive lanthanide metals to the Ln<sup>III</sup> oxidation state.<sup>[2]</sup> The electron affinity of *t*BuN=CHCH=N*t*Bu (DAB) enables facile oxidation of ytterbocenes [YbCp<sub>2</sub>(thf)<sub>2</sub>] (Cp = C<sub>5</sub>H<sub>5</sub>,<sup>[3]</sup> C<sub>5</sub>Me<sub>5</sub>,<sup>[4]</sup> C<sub>9</sub>H<sub>7</sub>,<sup>[5]</sup> CH<sub>2</sub>-1-C<sub>9</sub>H<sub>6</sub><sup>[5]</sup>), which can afford metallocene-type complexes [YbCp<sub>2</sub>(dad<sup>-</sup>)] that contain the radical-anionic diazabutadiene ligand. Investigation of the reactivity of the bulkier diazabutadiene 2,6-*i*Pr<sub>2</sub>C<sub>6</sub>H<sub>3</sub>-N=CH-CH=N-C<sub>6</sub>H<sub>3</sub>*i*Pr<sub>2</sub>-2,6

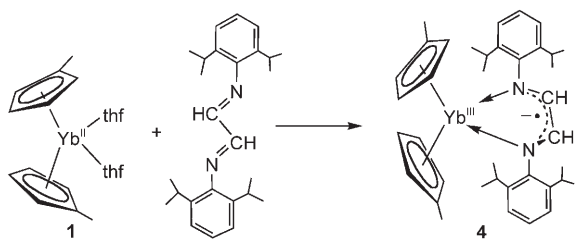
(DAD) towards the Yb<sup>II</sup> complexes [YbCp<sub>2</sub>(thf)<sub>2</sub>] (Cp = C<sub>9</sub>H<sub>7</sub>,<sup>[6]</sup> C<sub>13</sub>H<sub>9</sub><sup>[7]</sup>) has shown that the reactions of these compounds are driven by steric crowding in the coordination sphere of the ytterbium atom. Consequently, the reaction of DAD with the bis(indenyl) derivative [Yb(C<sub>9</sub>H<sub>7</sub>)<sub>2</sub>(thf)<sub>2</sub>] afforded the oxidation product [Yb(C<sub>9</sub>H<sub>7</sub>)<sub>2</sub>(dad<sup>-</sup>)],<sup>[6]</sup> whereas the reaction with the analogue [Yb(C<sub>13</sub>H<sub>9</sub>)<sub>2</sub>(thf)<sub>2</sub>], containing bulkier fluorenyl ligands, occurred through C-C coupling and formed an unusual Yb<sup>II</sup> complex [Yb{η<sup>5</sup>-C<sub>13</sub>H<sub>8</sub>C(=N-C<sub>6</sub>H<sub>3</sub>*i*Pr<sub>2</sub>-2,6)CH<sub>2</sub>NHC<sub>6</sub>H<sub>3</sub>*i*Pr<sub>2</sub>-2,6)<sub>2</sub>(thf)}].<sup>[7]</sup> To gain insight into the steric manipulation of the reductive reactivity of ytterbocenes in their reactions with diazabutadienes, we have explored the reactions of DAD with Yb<sup>II</sup> complexes that are similar in nature and structure, but contain different steric demands (controlled by the π-aromatic ligands coordinated to the ytterbium atom), namely, [YbCp\*<sub>2</sub>(thf)<sub>2</sub>] (Cp\* = C<sub>5</sub>MeH<sub>4</sub> (**1**), C<sub>5</sub>Me<sub>4</sub>H (**2**), C<sub>5</sub>Me<sub>5</sub> (**3**)).

## Results and Discussion

Reaction of DAD with complex **1** was carried out in THF at room temperature. After evaporation of the THF in vacuo, the solid residue was redissolved in hot toluene and recrystallised from hexane to afford wine-coloured crystals of [Yb(C<sub>5</sub>MeH<sub>4</sub>)<sub>2</sub>(dad)] (**4**) in 61 % yield (Scheme 1). Complex **4** is

[a] Prof. Dr. A. A. Trifonov, I. A. Borovkov, Dr. E. A. Fedorova, Dr. G. K. Fukin, Dr. N. O. Druzhkov, Prof. Dr. V. K. Cherkasov  
Institute of Organometallic Chemistry  
Russian Academy of Sciences, Tropinina 49  
603950, Nizhny Novgorod, GSP-445 (Russia)  
Fax: (+7)8312-621-497  
E-mail: trif@imoc.sinn.ru

[b] Dr. J. Larionova  
Laboratoire de Chimie Moléculaire et Organisation du Solide  
Batiment 17, Case Courrier 007, Place Eugene Bataillon  
34095 Montpellier Cedex 5 (France)



Scheme 1. Reaction of DAD with complex **1** to form complex **4**.

highly air- and moisture-sensitive, soluble in toluene and less soluble in hexane. Crystals suitable for single-crystal X-ray diffraction studies were obtained by slow cooling of a solution of **4** in hexane to  $-20^{\circ}\text{C}$ . The molecular structure of **4** is depicted in Figure 1, and crystal and structural refinement data are listed in Table 1.

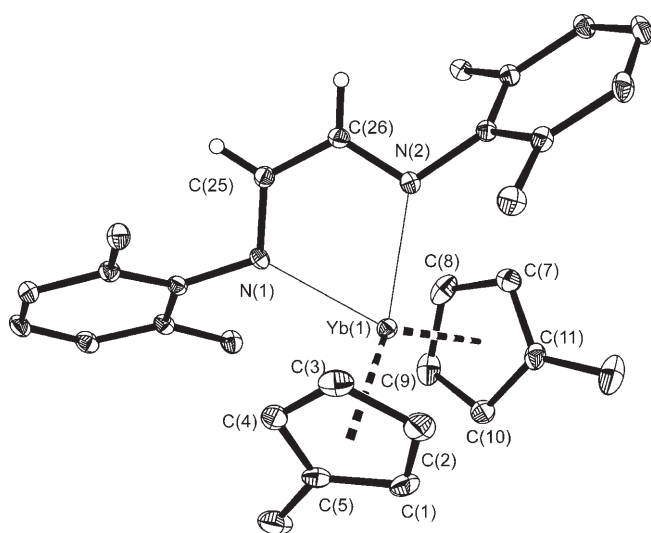


Figure 1. Molecular structure of complex **4**. The *iPr* groups of DAD are omitted. Selected distances [ $\text{\AA}$ ] and angles [ $^{\circ}$ ]: Yb–N(1) 2.3577(14), Yb–N(2) 2.3926(13), Yb–C(8) 2.5870(19), Yb–C(3) 2.5929(19), Yb–C(2) 2.594(2), Yb–C(7) 2.5945(18), Yb–C(9) 2.6197(19), Yb–C(1) 2.628(2), Yb–C(4) 2.6311(19), Yb–C(5) 2.6311(19), Yb–C(10) 2.6516(18), N(1)–C(25) 1.338(2), N(2)–C(26) 1.335(2), C(25)–C(26) 1.395(2); Cp<sub>Centre</sub>–Yb–Cp<sub>Centre</sub> 125.8(5), N(1)–Yb–N(2) 72.8(5).

In complex **4**, the ytterbium atom is  $\eta^5$ -coordinated by the two cyclopentadienyl rings and the two nitrogen atoms of the DAD ligand, and the complex adopts the geometry of a distorted tetrahedron. The average Yb–C (2.619(2)  $\text{\AA}$ ) and the Yb–Cp<sub>Centre</sub> (2.332(2), 2.331(2)  $\text{\AA}$ ) distances in **4** are shorter than those in the Yb<sup>II</sup> complex [Yb(C<sub>5</sub>MeH<sub>4</sub>)<sub>2</sub>(thf)] (Yb–C<sub>av</sub> = 2.76(3), 2.87(3), 2.91(3)  $\text{\AA}$ )<sup>[8]</sup> and are close to the values reported for the related mixed-ligand diazabutadiene Yb<sup>III</sup> derivatives [Yb(C<sub>5</sub>H<sub>5</sub>)(*t*BuNCHCHN*t*Bu)] (Yb–Cp<sub>Centre</sub> = 2.324(7), 2.334(4)  $\text{\AA}$ )<sup>[3]</sup> [YbCp<sub>2</sub>(*t*BuNCHCHN*t*Bu)] (Yb–C<sub>av</sub> = 2.69(4)  $\text{\AA}$  and Yb–Cp<sub>Centre</sub> = 2.414(2), 2.4009(18)  $\text{\AA}$ )<sup>[4]</sup> [Yb(C<sub>9</sub>H<sub>7</sub>)<sub>2</sub>(*t*BuNCHCHN*t*Bu)] (Yb–C<sub>av</sub> = 2.668(6)  $\text{\AA}$  and Yb–Cp<sub>Centre</sub> = 2.383(3), 2.376(3)  $\text{\AA}$ )<sup>[5]</sup> [Yb-

(C<sub>9</sub>H<sub>7</sub>)<sub>2</sub>(dad)] (Yb–C<sub>av</sub> = 2.663(4)  $\text{\AA}$  and Yb–Cp<sub>Centre</sub> = 2.3760(18)  $\text{\AA}$ )<sup>[6]</sup>. The shortening of the Yb–Cp<sub>Centre</sub> distances in **4** relative to those in **1** reflects the oxidation of the ytterbium atom to the Yb<sup>III</sup> state.<sup>[9]</sup> The two Yb–N bonds in **4** (2.3577(14) and 2.3926(13)  $\text{\AA}$ ) differ in their lengths but they lie in the region reported for related complexes [YbCp<sub>2</sub>(*t*BuNCHCHN*t*Bu)] (2.309(9) and 2.306(9)  $\text{\AA}$ )<sup>[3]</sup> [YbCp<sub>2</sub>(*t*BuNCHCHN*t*Bu)] (2.385(4) and 2.394(3)  $\text{\AA}$ )<sup>[4]</sup> [Yb(C<sub>9</sub>H<sub>7</sub>)<sub>2</sub>(*t*BuNCHCHN*t*Bu)] (2.318(5) and 2.335(5)  $\text{\AA}$ )<sup>[5]</sup> and [Yb(C<sub>9</sub>H<sub>7</sub>)<sub>2</sub>(dad)] (2.381(3)  $\text{\AA}$ )<sup>[6]</sup>. The Yb–N bond lengths in **4** are comparable to the lengths of the Yb<sup>III</sup>–N coordination bonds in the compounds [Yb(C<sub>5</sub>Me<sub>5</sub>)<sub>2</sub>(bipy)]<sup>+</sup>[Yb(C<sub>5</sub>Me<sub>5</sub>)<sub>2</sub>Cl<sub>2</sub>]<sup>–</sup> (2.37  $\text{\AA}$ )<sup>[10]</sup> [Yb(C<sub>5</sub>Me<sub>5</sub>)<sub>2</sub>(phen)]<sup>+</sup>[I]<sup>–</sup>(CH<sub>2</sub>Cl<sub>2</sub>) (2.36  $\text{\AA}$ )<sup>[10]</sup> and [YbCp<sub>2</sub>(HPzMe<sub>2</sub>)(PzMe<sub>2</sub>)] (HPzMe<sub>2</sub> = 3,5-dimethylpyrazole) (2.360(6), 2.414(6)  $\text{\AA}$ )<sup>[11]</sup> but are much longer than the covalent Yb<sup>III</sup>–N bonds in [Yb( $\eta^5$ -C<sub>9</sub>H<sub>7</sub>)<sub>2</sub>N(SiMe<sub>3</sub>)<sub>2</sub>] (2.160(5), 2.163(5)  $\text{\AA}$ )<sup>[12]</sup> [Yb( $\eta^5$ -C<sub>5</sub>H<sub>4</sub>Me)<sub>2</sub>NPh<sub>2</sub>] (2.216(5)  $\text{\AA}$ )<sup>[13]</sup> [Yb( $\eta^5$ -C<sub>5</sub>H<sub>4</sub>Me)<sub>2</sub>NPh<sub>2</sub>(thf)] (2.287(6)  $\text{\AA}$ )<sup>[13]</sup> and [Li(thf)<sub>4</sub>][Yb(NPh<sub>2</sub>)<sub>4</sub>] (2.188(9)–2.2401(9)  $\text{\AA}$ )<sup>[14]</sup>. The geometric parameters of the DAD ligand in **4** are noticeably different from the parent diazabutadiene and indicate its reduced radical-anionic character. An electron transfer to the LUMO of the ligand is expected to cause delocalization of the charge over the conjugated NCCN fragment and result in changes in the bond lengths. Compared with the N=C (1.266(3)  $\text{\AA}$ )<sup>[15]</sup> and C–C bond lengths (1.467(5)  $\text{\AA}$ )<sup>[15]</sup> of a neutral DAD molecule, the N=C bonds in the bound DAD ligand of **4** (1.338(2) and 1.335(2)  $\text{\AA}$ ) are substantially elongated and the C–C bond (1.395(2)  $\text{\AA}$ ) is shortened (close to the values of aromatic C–C bonds)<sup>[16]</sup>. The bonding in **4** is similar to that previously described for [SmCp<sub>2</sub>(*t*BuNCHCHN*t*Bu)]<sup>[2a]</sup> [YbCp<sub>2</sub>(*t*BuNCHCHN*t*Bu)]<sup>[3]</sup> and [YbCp<sub>2</sub>(*t*BuNCHCHN*t*Bu)]<sup>[4]</sup> and supports the radical-anionic character of the DAD ligand in **4**.

The measurements of the magnetic susceptibility ( $\chi_M$ ) in the temperature interval of 2–300 K were performed by using an applied field of 1000 Oe. The temperature dependences of  $1/\chi_M$  and the magnetic moment calculated as  $\mu = 2.828\sqrt{\chi_M T}$  are shown in Figure 2. The shapes of these curves are different from those normally observed for an

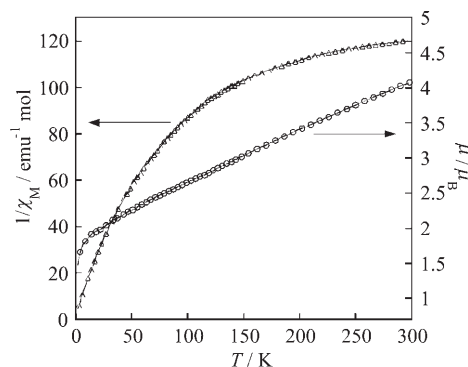


Figure 2. Thermal dependences of the magnetic moment ( $\mu$ ) (—○—) and  $1/\chi$  (—△—) for **4** performed by using an applied field of 1000 Oe.

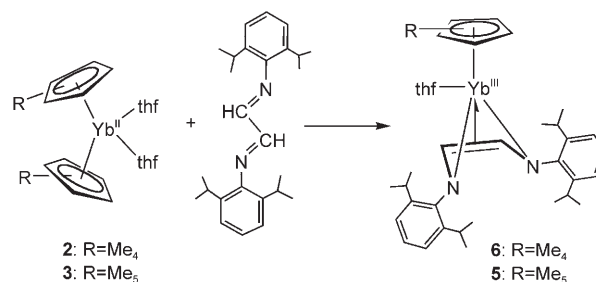
isolated Yb<sup>3+</sup> ion and a radical anion. The curve  $1/\chi_M = f(T)$  consists of three temperature domains: 2–25 K, 25–190 K, and 190–300 K. At high temperature (above  $T = 190$  K), the curve may be fitted by application of the Curie–Weiss law,  $1/\chi_M = (T - \theta)/C$ , with a Weiss constant ( $\theta$ ) of  $-260$  K and a Curie constant ( $C$ ) of  $2.069 \text{ emu K mol}^{-1}$ . At low temperature ( $T = 2\text{--}25$  K), the plot of  $1/\chi_M$  is directly proportional to the temperature and can be fitted by using the Curie law with a Curie constant of  $0.453 \text{ emu K mol}^{-1}$ . The curve  $\mu = f(T)$  decreases monotonically as the temperature decreases from  $4.06 \mu_B$  at 300 K to the value of  $1.64 \mu_B$  at 2 K.

The value of the magnetic moment ( $4.06 \mu_B$ ) observed at  $T = 300$  K suggests that the radical anion and both the ferro- and antiferromagnetic coupled states of Yb<sup>3+</sup> are present at room temperature. Indeed, this value is comparable to the theoretical Yb<sup>3+</sup> free-ion value for a  $^2F_{7/2}$  multiplet ( $4.5 \mu_B$ ).<sup>[17]</sup> As the temperature decreases, there is a progressive depopulation of the excited doublets and at low temperature (below  $T = 5$  K) the calculated free-ion value of the magnetic moment is  $3.8 \mu_B$ . In the case of the non-interacting ytterbium and radical-anion spins, the predicted magnetic moments, calculated as the square root of the sum of the squares of the individual moments of a ytterbium ion and an anion radical, should be  $4.8$  and  $4.2 \mu_B$  at high and low temperatures, respectively.<sup>[18]</sup> For a system involving electron-exchange coupling, the new term symbols can be calculated on the basis of linear combination of the  $^2F_{7/2}$  term of ytterbium and  $^2S_{1/2}$  term of the radical. For an antiferromagnetic interaction, this term is  $^{25}L_{J-1/2} = ^1F_3$ , whereas for a ferromagnetic interaction it is  $^{25+2}L_{J+1/2} = ^3F_4$ .<sup>[10]</sup> Therefore, the predicted low and high limiting values for the room temperature magnetic moment of ytterbium antiferro- or ferromagnetically coupled with an organic anion radical are  $3.46$  and  $5.59 \mu_B$ , respectively. However, as in the case of compound **4**, intermediate experimental values have also been observed for a few compounds containing Yb<sup>3+</sup> and radical anions, such as phthalocyanine or phenantrolyne, and were attributed to the simultaneous presence of both antiferro- and ferromagnetic interactions between Yb<sup>3+</sup> and radicals.<sup>[19,10]</sup>

The structural parameters, and spectroscopic and magnetic data of **4** provide evidence for the trivalent oxidation state of the ytterbium atom and the radical-anionic character of the DAD ligand. The complex  $[\text{Yb}(\text{C}_5\text{Me}_4\text{H})_2(\text{thf})_2]$  reacts with DAD as a one-electron reductant.

The reductive reactivity of ytterbocenes in their reactions with DAD has been found to be strongly dependent on steric crowding in the coordination sphere of the ytterbium atom. However, the interaction of ytterbocene  $[\text{Yb}(\text{C}_5\text{Me}_5)_2(\text{thf})_2]$  (**3**), containing the bulkier pentamethylcyclopentadienyl ligand, with DAD under similar conditions has resulted in elimination of one Cp\* ring and formation of the Yb<sup>III</sup> mono(cyclopentadienyl) complex  $[\text{Yb}(\text{C}_5\text{Me}_5)(\text{dad})(\text{thf})]$  (**5**) (Scheme 2).

Recently we reported that the reaction of DAD with the bis(flourenyl) derivative of  $[\text{Yb}(\text{C}_{13}\text{H}_9)_2(\text{thf})_2]$  occurs through coupling of the allylic-carbon atom of the fluorenyl ligand with one of the imino-carbon atoms of the diazadiene



Scheme 2. Reaction of DAD with complex **2** or **3** to form complex **6** or **5**, respectively.

and results in Yb<sup>III</sup> compound  $[\text{Yb}(\eta^5\text{-C}_{13}\text{H}_8\text{C}=\text{N}(2,6\text{-}i\text{Pr}_2\text{C}_6\text{H}_3))\text{CH}_2\text{NHC}_6\text{H}_5\{2,6\text{-}i\text{Pr}_2\})_2(\text{thf})]$ .<sup>[7]</sup> This reaction can be regarded as a useful synthetic method for functionalising the fluorenyl ligands. Analogously, we postulated that the tetramethylcyclopentadienyl ligand of complex **2**  $[\text{Yb}(\text{C}_5\text{Me}_4\text{H})_2(\text{thf})_2]$  contains a carbon atom susceptible to C–C bond formation. Nevertheless, complex  $[\text{Yb}(\text{C}_5\text{Me}_4\text{H})(\text{dad})(\text{thf})]$  (**6**), similar to **5**, was isolated from the reaction of **2** with DAD (Scheme 2).

Complexes **5** (yellow-green crystals) and **6** (brown-green crystals) are highly air- and moisture-sensitive, soluble in toluene and less soluble in hexane. Crystals suitable for single-crystal X-ray diffraction studies were obtained by slow condensation of hexane into solution of **5** in THF at room temperature. Compound **5** crystallises as a solvate  $[\text{Yb}(\text{C}_5\text{Me}_5)(\text{dad})(\text{thf})] \cdot (\text{C}_6\text{H}_{14})_{0.33} \cdot (\text{thf})_{0.67}$ . The unit cell of compound **5** contains three crystallographically independent molecules. Monocrystalline samples of **6** suitable for single-crystal X-ray diffraction studies were obtained by slow concentration of the solution of **6** in hexane at room temperature. The molecular structures of **5** and **6** are depicted in Figures 3 and 4 respectively, and crystal and structural refinement data are listed in Table 1.

The X-ray crystal structure determinations of **5** and **6** have revealed that these complexes have unusual structures. The coordination sphere of the Yb<sup>III</sup> atom in **5** and **6** is braced by a  $\eta^5$ -coordinated Cp\* ligand, the dianion of diazabutadiene ( $\eta^4$ -coordinated) and one THF molecule (Figures 3 and 4).

The average Yb–C(Cp\*) bond lengths in complexes **5** and **6** (2.589 and 2.586 Å) are much shorter than their corresponding values in the Yb<sup>III</sup> complex  $[\text{YbCp}^*_2(\text{py})_2]$  (2.74 Å: py = pyridine)<sup>[20]</sup> and comparable to those in related Yb<sup>III</sup> complexes  $[\text{Yb}(\text{C}_5\text{Me}_5)_2(\text{L})\text{X}]$  (2.628–2.65 Å, X = Hal, L = THF).<sup>[21]</sup> The geometry of the planar NCCN fragment (deviation from the plane  $\approx 0.001$  Å) in **5** and **6** is consistent with the dianionic character of the DAD ligand. The N–C bonds in the DAD dianion of **5** (1.409(5) and 1.387(6) Å) and **6** (1.406(5) and 1.411(6) Å) are substantially elongated, whereas the C–C bonds (**5**: 1.348(7) Å, **6**: 1.360(6) Å) are shortened, relative to the N=C (1.266(3) Å)<sup>[15]</sup> and C–C bond lengths (1.467(5) Å)<sup>[15]</sup> in the free DAD molecule. The C–C bond lengths are close to the values of C=C double bond lengths.<sup>[16]</sup> The bonding situation within the DAD

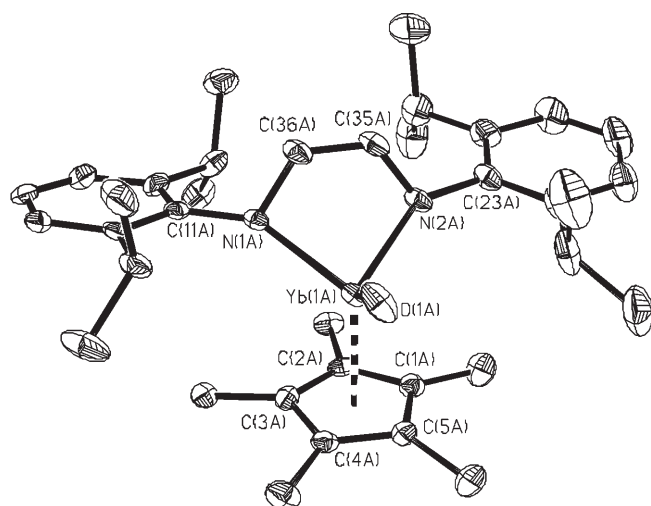


Figure 3. Molecular structure of complex **5** (one crystallographically independent molecule). The CH<sub>2</sub> groups of the THF ligand and the hydrogen atoms of the DAD ligand are omitted. Selected distances [Å] and angles [°]: Yb(1A)–N(2A) 2.136(3), Yb(1A)–N(1A) 2.145(3), Yb(1A)–O(1A) 2.305(3), Yb(1A)–C(3A) 2.566(4), Yb(1A)–C(2A) 2.570(4), Yb(1A)–C(1A) 2.585(4), Yb(1A)–C(4A) 2.608(4), Yb(1A)–C(5A) 2.618(5), Yb(1A)–C(35A) 2.618(4), Yb(1A)–C(36A) 2.628(5), N(1A)–C(36A) 1.409(5), N(2A)–C(35A) 1.388(6), C(35A)–C(36A) 1.348(7); N(2A)–Yb(1A)–N(1A) 85.1(1), Cp<sub>Centre</sub>–Yb(1)–Cp<sub>Centre</sub> 142.2(1).

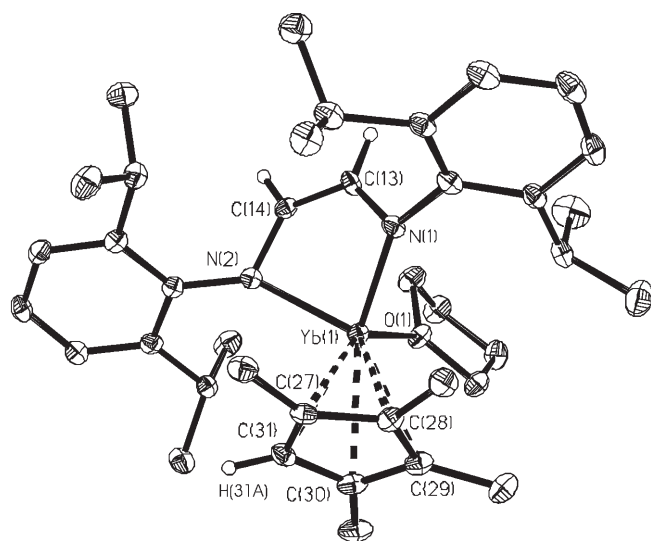


Figure 4. Molecular structure of complex **6**. Selected distances [Å] and angles [°]: Yb(1)–N(2) 2.141(4), Yb(1)–N(1) 2.148(3), Yb(1)–O(1) 2.305(3), Yb(1)–C(31) 2.555(4), Yb(1)–C(27) 2.558(4), Yb(1)–C(28) 2.586(4), Yb(1)–C(30) 2.609(4), Yb(1)–C(14) 2.622(4), Yb(1)–C(29) 2.622(4), Yb(1)–C(13) 2.629(5), N(1)–C(13) 1.411(6), N(2)–C(14) 1.406(5); N(2)–Yb(1)–N(1) 85.70(13), Cp<sub>Centre</sub>–Yb(1)–Cp<sub>Centre</sub> 141.5(1).

ligand and its coordination mode in **5** and **6** are different from those observed for the radical-anionic ligand (**4**). The C=C bond of a doubly reduced ene-diamido moiety NCCN also participates in metal-ligand bonding. η<sup>2</sup>-Coordination of the ene-diamido moiety to the Yb atom results in short Yb–C contacts (**5**: 2.628(5), 2.618(4) Å; **6**: 2.622(4), 2.629(5) Å).

Table 1. Crystallographic data and structure refinement details for **4**, **5** and **6**.

	<b>4</b>	<b>5</b>	<b>6</b>
formula	C <sub>38</sub> H <sub>50</sub> N <sub>2</sub> Yb	C <sub>44.5</sub> H <sub>69</sub> N <sub>2</sub> O <sub>1.67</sub> Yb	C <sub>39</sub> H <sub>57</sub> N <sub>2</sub> OYb
M <sub>r</sub>	707.84	831.72	742.91
T [K]	100(2)	100(2)	100(2)
λ [Å]	0.71073	0.71073	0.71073
crystal system	monoclinic	monoclinic	monoclinic
space group	P2(1)/n	P2(1)/n	P2(1)/n
unit cell dimensions			
a [Å]	9.7966(6)	10.8252(6)	16.5331(11)
b [Å]	20.6075(12)	35.6896(18)	11.4198(7)
c [Å]	17.0649(10)	33.9278(17)	19.1959(13)
β [°]	101.6170(10)	93.2570(10)	100.4490(10)
V [Å <sup>3</sup> ]	3374.5(3)	13086.7(12)	3564.2(4)
Z	4	12	4
ρ <sub>calcd</sub> [g cm <sup>-3</sup> ]	1.393	1.266	1.384
μ [mm <sup>-1</sup> ]	2.798	2.178	2.655
F(000)	1448	5200	1532
crystal size [mm]	0.25 × 0.16 × 0.12	0.15 × 0.10 × 0.08	0.15 × 0.11 × 0.04
θ range [°]	1.98–29.01	1.66–26.00	1.80–24.00
index ranges	–13 ≤ h ≤ 13 –28 ≤ k ≤ 28 –23 ≤ l ≤ 23	–13 ≤ h ≤ 13 –44 ≤ k ≤ 44 –41 ≤ l ≤ 41	–18 ≤ h ≤ 18 –12 ≤ k ≤ 13 –21 ≤ l ≤ 21
reflns collected	35 313	111 034	25 056
independent	8948	25 718	5574
reflns			
R <sub>int</sub>	0.0348	0.0446	0.0637
completeness to θ	99.5	99.9	99.9
data/restraints/parameters	8948/13/570	25 718/108/1378	5574/0/388
GoF on F <sup>2</sup>	1.036	1.259	0.984
final R indices [I > 2σ(I)]			
R1	0.0251	0.0664	0.0356
wR2	0.0538	0.1350	0.0797
R indices (all data)			
R1	0.0356	0.0797	0.0560
wR2	0.0566	0.1389	0.0855
largest diff. peak/hole [e Å <sup>-3</sup> ]	1.335/–0.423	1.715/–1.750	1.788/–0.783

To the best of our knowledge, this is the first example of terminal coordination by a diazabutadiene dianion to a lanthanide atom.<sup>[22]</sup> The values of Cp<sub>Centre</sub>–Yb–dad<sub>Centre</sub> angles in complexes **5** and **6** (142.2(1) and 141.5(1)° respectively) are slightly larger than the Cp<sub>Centre</sub>–Yb–Cp<sub>Centre</sub> angles reported for metallocene-type derivatives of trivalent ytterbium [Yb(C<sub>5</sub>Me<sub>5</sub>)<sub>2</sub>(L)X] (134.9–136.3°).<sup>[21]</sup> Complexes **5** and **6** can be regarded as novel Yb<sup>III</sup> mixed-ligand bent-sandwich complexes.

The UV-visible spectra of **5** and **6** in THF show strong absorptions at λ = 285 and 290 nm respectively, which correspond well with the strong band of (Li<sup>+</sup>)<sub>2</sub>(dad<sup>2-</sup>) in THF at λ = 290 nm. This evidence supports the hypothesis for a dianionic DAD ligand in solution (Figure 5).

To examine the possibility of the existence and temperature-induced transformation of the different redox tautomers of complex **5**, namely, [Yb<sup>III</sup>(C<sub>5</sub>Me<sub>5</sub>)(dad<sup>2-</sup>)(thf)] and [Yb<sup>II</sup>(C<sub>5</sub>Me<sub>5</sub>)(dad<sup>-</sup>)(thf)], an investigation of magnetic properties of **5** has been performed. An investigation of the redox tautomerism of complex **5** was expected to be of in-

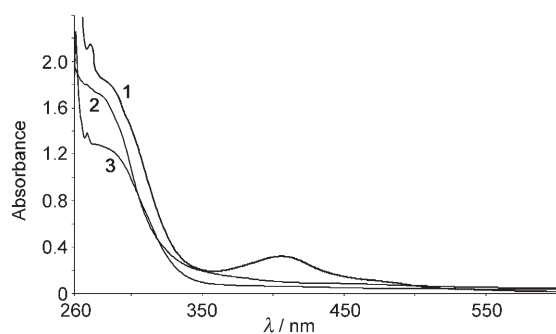


Figure 5. UV/Vis spectra: (Li<sup>+</sup>)<sub>2</sub>(dad)<sup>2-</sup> (**1**) in THF, [Yb(C<sub>5</sub>Me<sub>5</sub>)(dad)(thf)] (**2**) in THF, and [Yb(C<sub>5</sub>Me<sub>4</sub>H)(dad)(thf)] (**3**) in THF.

terest as both of the forms contain a single paramagnetic center, and spin antiferromagnetic coupling can be excluded. The temperature dependence of the magnetic susceptibility was studied by using an applied field of 500 Oe (Figure 6).

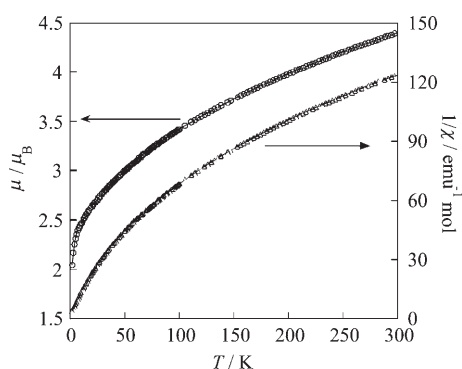


Figure 6. Thermal dependences of magnetic moment ( $\mu$ ) (○) and  $1/\chi_M$  (△) for **5** performed with an applied field of 500 Oe.

The curve  $1/\chi_M = f(T)$  consists of three temperature domains: 2–25 K, 25–150 K, and 150–300 K. At high temperature (above  $T = 150$  K), the curve may be fitted by using the Curie–Weiss law,  $1/\chi_M = (T - \theta)/C$  to give a Weiss constant of  $-240$  K and a Curie constant of  $3.239$  emu K mol<sup>-1</sup>.

The value of the Weiss constant found for complex **5** is lower than the one observed for isolated metallocenes and other compounds of Yb<sup>3+</sup>, which are usually in the range  $-20$  to  $-100$  K. The magnetic moment at  $T = 300$  K, calculated as  $\mu = 2.828(\chi_M T)^{1/2}$ , is  $4.41 \mu_B$ , which is close to the calculated free Yb<sup>3+</sup> ion value for a <sup>2</sup>F<sub>7/2</sub> multiplet.<sup>[17]</sup> In the low-temperature domain ( $T = 2$ – $25$  K), the plot of  $1/\chi_M$  is linearly related to temperature. The fitting by means of the Curie–Weiss law provides Weiss and Curie constants of  $-1.89$  K and of  $0.664$  emu K mol<sup>-1</sup>, respectively. The calculated value of the magnetic moment at  $T = 2$  K of  $2.03 \mu_B$  is too low for Yb<sup>III</sup> and is more compatible with the magnetic moments observed for organic radical anions with spin  $S = 1/2$  ( $1.73 \mu_B$ ). The field dependence of the magnetization performed at  $T = 2$  K for sample **5** was satisfactorily fitted by using the Brillouin function with  $S = 1/2$  (Figure 7). However,

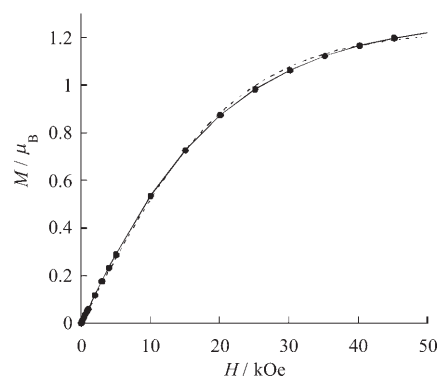
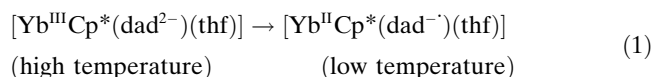


Figure 7. Field dependence of magnetization for sample **5** (●) performed at 2 K. Brillouin function fitting with  $S = 1/2$  is shown as a dashed line.

the value of the saturation magnetization at 50 kOe of  $1.21 \mu_B$  is slightly higher than the expected value given for a free radical that has  $S = 1/2$  and  $g = 2.0023$ . Such magnetic behaviour may be attributed to temperature-induced redox-tautomeric transformations of two forms of complex **5** [Eq. (1)].



The ESR spectroscopic investigation of solutions of **5** in mixtures of toluene/CH<sub>2</sub>Cl<sub>2</sub> (95:5) over a wide range of temperatures has shown that the signal can be observed only at temperatures below 14 K. The temperature decrease from 14 to 2.9 K results in monotonous transformation of the signal in the ESR spectrum of **5**. At  $T = 2.9$  K the spectrum contains (in the region of  $\approx 130$  mT) a complex set of lines, which can be attributed to the hyperfine splitting of magnetic isotopes <sup>171</sup>Yb (16.20%;  $5/2$ ;  $\mu_N = 0.4926$ ); <sup>173</sup>Yb (14.40%;  $1/2$ ;  $\mu_N = -0.677$ ).<sup>[23]</sup> The spectrum also contains a low-intensity transition at 335 mT ( $g_{\text{eff}} \approx 2.00$ ,  $\Delta H \approx 6$  mT) that can be attributed to an admixture of the DAD radical anion.

## Conclusion

The reactions of the ytterbocenes [YbCp\*<sub>2</sub>(thf)<sub>2</sub>] (Cp\* = C<sub>5</sub>MeH<sub>4</sub>, C<sub>5</sub>Me<sub>4</sub>H, C<sub>5</sub>Me<sub>5</sub>) with the sterically demanding diazabutadiene 2,6-*i*Pr<sub>2</sub>C<sub>6</sub>H<sub>3</sub>-N=CH-CH=N-C<sub>6</sub>H<sub>3</sub>*i*Pr<sub>2</sub>-2,6 have been found to be strongly dependent on the steric crowding within the coordination sphere of the ytterbium atom. The less sterically crowded ytterbocene [Yb-(C<sub>5</sub>MeH<sub>4</sub>)<sub>2</sub>(thf)<sub>2</sub>] acts as a one-electron reductant and its reaction afforded a bis(cyclopentadienyl) Yb<sup>III</sup> derivative containing a DAD radical anion [Yb(C<sub>5</sub>MeH<sub>4</sub>)<sub>2</sub>(dad<sup>-</sup>)]. The more sterically crowded compounds [YbCp\*<sub>2</sub>(thf)<sub>2</sub>] (Cp\* = C<sub>5</sub>Me<sub>5</sub>, C<sub>5</sub>Me<sub>4</sub>H) act as two-electron reductants and their reactions occur through the elimination of one Cp\* ring and result in the formation of novel Yb<sup>III</sup> bent-sandwich com-

plexes, [YbCp\*(dad)(thf)]. The dianion of diazabutadiene in [YbCp\*(dad)(thf)] has an unusual terminal  $\eta^4$ -coordination mode. Clearly, complexes [YbCp\*<sub>2</sub>(thf)<sub>2</sub>] demonstrate sterically induced reductive reactivity<sup>[24]</sup> and double reduction of DAD becomes possible as a result of oxidation of the Yb<sup>II</sup> to Yb<sup>III</sup> and oxidation of one Cp\* anion. The complexes of the form [YbCp\*(dad)(thf)] can be considered as novel Yb<sup>III</sup> mixed-ligand bent-sandwich complexes.

## Experimental Section

**General remarks:** All procedures were performed under vacuum by using standard Schlenk techniques. After drying over KOH, THF was distilled from sodium benzophenone ketyl prior to use. Hexane and toluene were purified by distillation from sodium/triglyme benzophenone ketyl or CaH<sub>2</sub>. Deuterated benzene was dried with sodium benzophenone ketyl and vacuum-transferred. [Yb(C<sub>5</sub>Me<sub>5</sub>)<sub>2</sub>(thf)<sub>2</sub>]<sup>[25]</sup> and [Yb(C<sub>5</sub>Me<sub>4</sub>H)<sub>2</sub>(thf)<sub>2</sub>]<sup>[8]</sup> were obtained by following the published synthetic procedures. All other commercially available chemicals were used after the appropriate purification. IR spectra were recorded by using a "Specord M80" instrument with samples as Nujol mulls. The UV/VIS spectra were recorded in evacuated quartz cuvettes by using a Perkin-Elmer Lambda 25 spectrophotometer. Magnetic susceptibility data were collected by using a Quantum Design MPMS-XL SQUID magnetometer working in the temperature range of 1.8–300 K and the magnetic field range of 0–50 kOe. The measurements were performed under an argon atmosphere. The data were corrected for the sample holder and the diamagnetism contributions calculated from Pascal constants.<sup>[26]</sup> Lanthanide metal analyses were carried out by means of complexometric titration. Elemental analyses were performed by the Microanalytical laboratory of the Institute of Organometallic Chemistry of RAS.

**Synthesis of [Yb(C<sub>5</sub>MeH)<sub>2</sub>(dad)(thf)] (4):** A solution of DAD (0.70 g, 1.90 mmol) in THF (5 mL) was added to a solution of [Yb(C<sub>5</sub>MeH)<sub>2</sub>(thf)<sub>2</sub>] (0.90 g, 1.90 mmol) in THF (10 mL). The reaction mixture was stirred for 0.5 h at 40 °C. After the removal of THF in vacuo, toluene (15 mL) was added and the solution was heated to 60 °C for 1.5 h. The toluene was then evaporated in vacuo. Recrystallisation of the solid residue from hexane (–20 °C) gave **4** as wine-coloured crystals (0.81 g, 61%). The crystals were washed with cold hexane and dried in vacuo at RT for 45 min. IR (Nujol, KBr):  $\tilde{\nu}$  = 3050 (w), 1627 (s), 1585 (s), 1250 (s), 1210 (s), 755 cm<sup>-1</sup> (s); elemental analysis calcd (%) for C<sub>38</sub>H<sub>50</sub>N<sub>2</sub>Yb (707.8): C 64.51, H 7.07, Yb 24.45; found: C 64.04, H 6.69, Yb 24.61.

**Synthesis of [Yb(C<sub>5</sub>Me<sub>5</sub>)(dad)(thf)] (5):** A solution of DAD (0.45 g, 1.20 mmol) in THF (10 mL) was added to a solution of [Yb(C<sub>5</sub>Me<sub>5</sub>)<sub>2</sub>(thf)<sub>2</sub>] (0.71 g, 1.20 mmol) in THF (10 mL). The reaction mixture was stirred for 0.5 h at 40 °C. THF was evaporated in vacuo, toluene (25 mL) was added, and the reaction mixture was stirred at 60 °C for 1.5 h. The toluene was then evaporated in vacuo. Recrystallisation of the solid residue from a THF/hexane mixture gave **5** as yellow-green crystals (0.42 g, 47%). The crystals were washed with cold hexane and dried in vacuo at RT for 1 h. IR (Nujol, KBr):  $\tilde{\nu}$  = 3050 (w), 1627 (s), 1585 (s), 1250 (s), 1210 (s), 1087 (s), 854 (s), 755 cm<sup>-1</sup> (s); elemental analysis calcd (%) for C<sub>40</sub>H<sub>50</sub>N<sub>2</sub>OYb (756.4): C 63.51, H 7.79, Yb 22.87; found: C 63.07, H 7.47, Yb 23.00.

**Synthesis of [Yb(C<sub>5</sub>Me<sub>4</sub>H)(dad)(thf)] (6):** A solution of DAD (0.56 g, 1.49 mmol) in THF (5 mL) was added to a solution of [Yb(C<sub>5</sub>Me<sub>4</sub>H)<sub>2</sub>(thf)<sub>2</sub>] (0.84 g, 1.49 mmol) in THF (10 mL). The reaction mixture was stirred for 0.5 h at 40 °C. THF was evaporated in vacuo, toluene (20 mL) was added, and the reaction mixture was stirred at 60 °C for 1.5 h. The toluene was then evaporated in vacuo. Recrystallisation of the solid residue from hexane (–20 °C) gave **6** as brown-green crystals (0.64 g, 58%). IR (Nujol, KBr):  $\tilde{\nu}$  = 3050 (w), 1627 (s), 1585 (s), 1250 (s), 1210 (s), 1087 (s), 854 (s), 755 cm<sup>-1</sup> (s); elemental analysis calcd (%) for C<sub>39</sub>H<sub>57</sub>N<sub>2</sub>OYb (742.9): C 63.09, H 7.67, Yb 23.30; found: C 62.77, H 7.21, Yb 23.35.

**X-ray crystallographic study:** The data were collected on a SMART APEX diffractometer (graphite-monochromated MoK $\alpha$  radiation,  $\omega$ - and  $\theta$ -scan technique,  $\lambda$  = 0.71073 Å). The structures were solved by direct methods and were refined on  $F^2$  by using the SHELXTL<sup>[27]</sup> package. All non-hydrogen atoms were refined anisotropically and the hydrogen atoms in **4** were found from the Fourier syntheses of the electron density and were refined isotropically, whereas hydrogen atoms in **5** and **6** were placed in calculated positions and were refined in the riding model. SADABS<sup>[28]</sup> was used to perform area-detector scaling and absorption corrections.

## Acknowledgements

This work was supported by the Russian Foundation of Basic Research (grants 05-03-32390, 06-03-32728-a, 06-03-81005Bel). A.T. acknowledges the Federal Science and Innovation Agency, the Russian Academy of Science (RAS), and the RAS Chemistry and Material Science Division for the 02.445.11.7365 contract, and the Grant of the President of the Russian Federation supporting scientific schools (No. 8017.2006.3). A.T. thanks the Russian Foundation for science support. J.L. thanks the University of Montpellier II, CNRS and network of excellence MAGMA-NET for financial support.

- [1] a) H. tom Dieck, I. W. Renk, *Chem. Ber.* **1971**, *104*, 110–130; b) H. tom Dieck, K.-D. Franz, F. Hoffmann, *Chem. Ber.* **1975**, *108*, 163–173; c) J. Reinhold, R. Benedix, P. Birner, H. Hennig, *Inorg. Chim. Acta* **1979**, *33*, 209–213.
- [2] a) A. Recknagel, M. Noltemeyer, F. T. Edelmann, *J. Organomet. Chem.* **1991**, *410*, 53–61; b) M. N. Bochkarev, A. A. Trifonov, F. G. N. Cloke, C. I. Dalby, P. T. Matsunaga, R. A. Andersen, H. Schumann, J. Loebel, H. Hemling, *J. Organomet. Chem.* **1995**, *486*, 177–182.
- [3] A. A. Trifonov, E. N. Kirillov, M. N. Bochkarev, H. Schumann, S. Muehle, *Russ. Chem. Bull.* **1999**, *48*, 382–384.
- [4] A. A. Trifonov, Yu. A. Kurskii, M. N. Bochkarev, S. Muehle, S. Dechert, H. Schumann, *Russ. Chem. Bull.* **2003**, *52*, 601–606.
- [5] A. A. Trifonov, E. A. Fedorova, V. N. Ikorskii, S. Dechert, H. Schumann, M. N. Bochkarev, *Eur. J. Inorg. Chem.* **2005**, 2812–2818.
- [6] A. A. Trifonov, E. A. Fedorova, G. K. Fukin, V. N. Ikorskii, Yu. A. Kurskii, S. Dechert, H. Schumann, M. N. Bochkarev, *Russ. Chem. Bull.* **2004**, *53*, 2736–2743.
- [7] A. A. Trifonov, E. A. Fedorova, G. K. Fukin, N. O. Druzhkov, M. N. Bochkarev, *Angew. Chem.* **2004**, *116*, 5155–5158; *Angew. Chem. Int. Ed.* **2004**, *43*, 5045–5048.
- [8] H. A. Zinnen, J. J. Pluth, W. J. Evans, *J. Chem. Soc. Chem. Commun.* **1980**, 810–812.
- [9] R. D. Shannon, *Acta Crystallogr., Sect A* **1976**, *32*, 751–767.
- [10] M. Schulz, J. M. Boncella, D. J. Berg, T. Don Tilley, R. A. Andersen, *Organometallics* **2002**, *21*, 460–472.
- [11] X. Zhou, Z. Huang, R. Cai, L.-B. Zhang, L.-X. Zhang, X. Huang, *Organometallics* **1999**, *18*, 4128–4133.
- [12] E. Sheng, S. Wang, G. Yang, S. Zhou, L. Cheng, K. Zhang, Z. Huang, *Organometallics* **2003**, *22*, 684–692.
- [13] Y. Wang, Q. Shen, F. Xue, K. Tu, *J. Organomet. Chem.* **2000**, *598*, 359–364.
- [14] W.-K. Wong, L. Zhang, F. Xue, T. C. W. Mak, *Polyhedron* **1997**, *16*, 345–347.
- [15] T. V. Laine, M. Klinga, A. Maaninen, E. Aitola, M. Leskelä, *Acta Chem. Scand.* **1999**, *53*, 968–973.
- [16] F. A. Allen, O. Konnard, D. G. Watson, L. Brammer, G. Orpen, R. Taylor, *J. Chem. Soc. Perkin Trans. 1* **1987**, 1–19.
- [17] R. D. L. Carlin, *Magnetochemistry*, Springer, Berlin, **1986**.
- [18] D. J. Berg, J. M. Boncella, R. A. Andersen, *Organometallics* **2002**, *21*, 4622–4631.

- [19] K. L. Trojan, J. L. Kendall, K. D. Kepler, W. E. Hatfield, *Inorg. Chim. Acta* **1992**, 198–200, 795–803.
- [20] T. D. Tilley, R. A. Andersen, B. Spencer, A. Zalkin, *Inorg. Chem.* **1982**, 21, 2647–2649.
- [21] a) P. L. Watson, T. H. Tulip, I. Williams, *Organometallics* **1990**, 9, 1999–2009; b) T. D. Tilley, R. A. Andersen, A. Zalkin, *Inorg. Chem.* **1983**, 22, 856–859.
- [22] For example, see: a) H. Görls, B. Neumüller, A. Scholz, J. Scholz, *Angew. Chem.* **1995**, 107, 732–735; *Angew. Chem. Int. Ed. Engl.* **1995**, 34, 673–676; b) A. A. Trifonov, L. N. Zakharov, M. N. Bochkarev, Yu. T. Struchkov, *Izv. Akad. Nauk, Ser. Khim.* **1994**, 148–150; c) A. A. Trifonov, E. A. Fedorova, G. K. Fukin, E. V. Baranov, N. O. Druzhkov, M. N. Bochkarev, *Chem. Eur. J.* **2006**, 12, 2752–2757.
- [23] B. A. Goodman, J. B. Raynor in *Advances in Inorganic and Radiochemistry, Vol. 13* (Eds.: H. J. Emeléus, A. G. Sharpe), Academic Press, NY and London, **1970**, pp. 136–362.
- [24] a) W. J. Evans, B. L. Davis, *Chem. Rev.* **2002**, 102, 2119–2136; b) W. J. Evans, *J. Organomet. Chem.* **2002**, 647, 2–11.
- [25] P. L. Watson, *J. Chem. Soc., Chem. Commun.* **1980**, 652.
- [26] E. A. L. Boudreaux, N. Mulay, *Theory and Applications of Molecular Paramagnetism*, Wiley, NY, **1976**.
- [27] Bruker SMART (version 5.625): Bruker Molecular Analysis Research Tool, Bruker AXS, Madison, Wisconsin (USA), **2000**.
- [28] SADABS (version 2.01): G. M. Sheldrick, Bruker/Siemens Area Detector Absorption Correction Program, Bruker AXS, Madison, Wisconsin (USA), **1998**.

Received: October 18, 2006

Published online: March 15, 2007